

On the Protonation of Water

Andras Bodi, József Csontos, Mihály Kállay, Sampada Borkar, Bálint Sztáray*

*Correspondence to: bsztaray@pacific.edu.

Electronic Supplementary Information

Figure S1, Scheme S1, Equation S1 and Tables S1–4

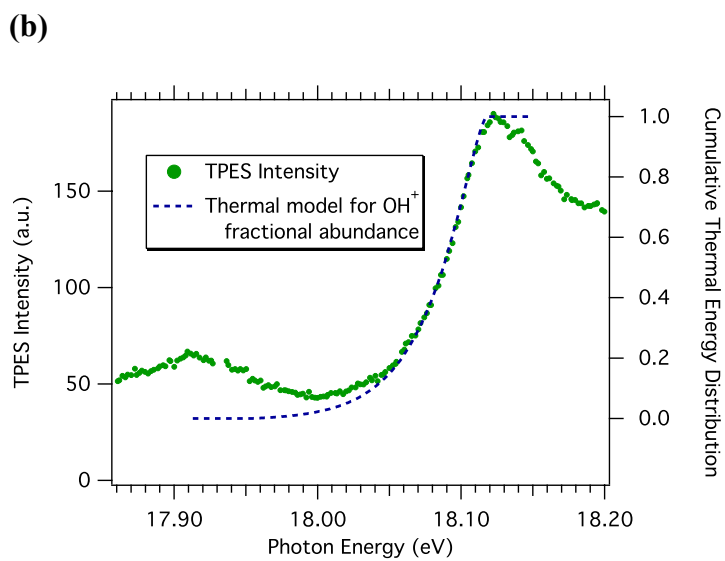
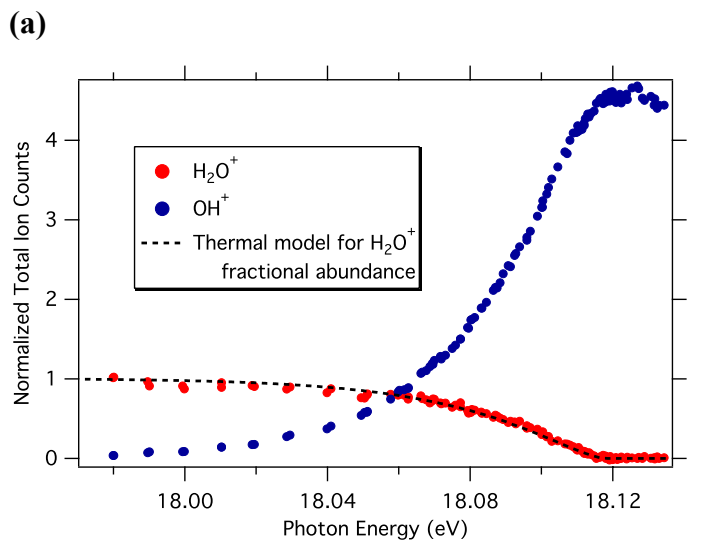
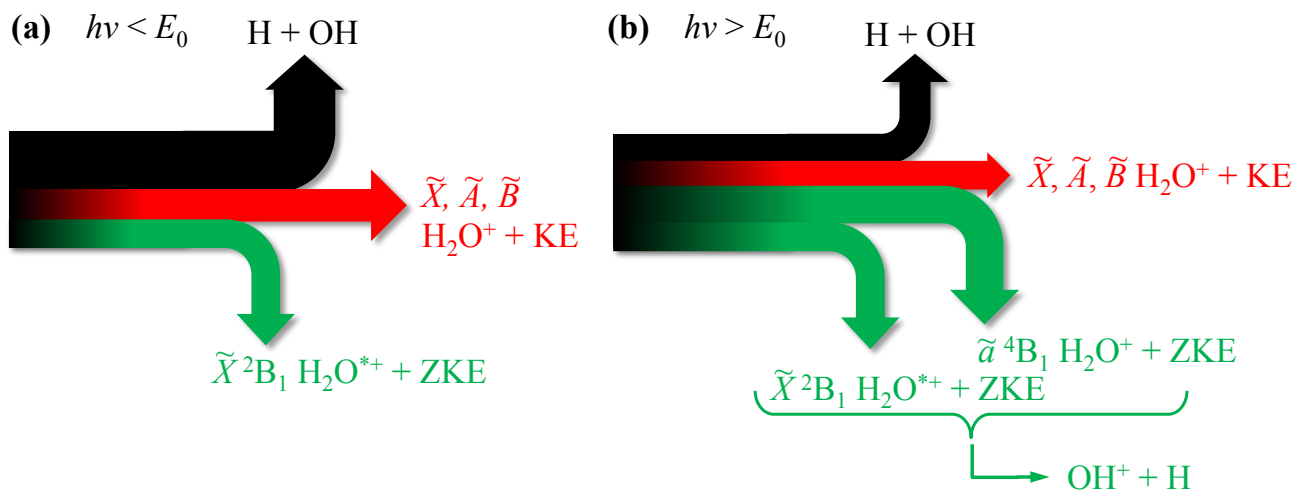


Fig. S1. (a) Absolute ion intensities vs. the modeled breakdown curve showing normal behavior for the H_2O^+ and enhanced photoionization cross section producing OH^+ ; **(b)** Threshold Photoelectron Spectrum (TPES) of room-temperature water along with the modeled breakdown curve (modeled relative ion abundance of OH^+).



Scheme S1. Radiationless relaxation pathways after photoabsorption in water, close to the H-loss dissociative photoionization threshold. Both below (a) and above (b) the threshold, the neutral dissociation products, H + OH, can be formed. Kinetic energy electrons are also emitted with a distribution determined by the photoelectron spectrum in non-resonant photoionization (red), and can initially yield the corresponding water ions in the energetically allowed, first three doublet ion states. Threshold photoionization (green) in the \tilde{B} band takes place via the Rydberg series converging to \tilde{B}^2B_2 ion states and finally yields rovibrationally excited, but electronically ground state $\tilde{X} H_2O^+$ ions. These are stable final products below threshold (a) and dissociate to form $OH^+ + H$ above threshold (b). Above threshold, the short-lived neutrals may also decay to \tilde{a}^4B_1 quartet ions, which then dissociate to the same $OH^+ + H$ products, and this latter channel is responsible for the increase in the threshold photoionization cross section.

Equation S1. Modified Eq. (4) to take preferential dissociative photoionization into account.

$$BD_d(h\nu) = \frac{f \cdot \int_{E_0-IE}^{+\infty} P_i(E, h\nu)}{\int_0^{E_0-IE} P_i(E, h\nu) + f \cdot \int_{E_0-IE}^{+\infty} P_i(E, h\nu)},$$

where BD_d is the fractional abundance of the daughter ion, E_0 the dissociative photoionization onset, IE the adiabatic ionization energy, P_i the energy distribution of the parent ion, and f is the preferential dissociative photoionization factor. Figure S1a–b also shows that the TPES, as well as the individual absolute threshold ionization ion yields are well described by this approach.

Supplementary Tables

Table S1. Theoretical estimates for the O–H bond length and the H–O–H bond angle in H₂O. The best estimates are obtained as the sum of the boldfaced values. Bond lengths and angles are given in Ångströms and degrees, respectively.

Basis set	$P_{\text{DKH/CCSD(T)}}$		ΔP_{T}		$\Delta P_{(\text{Q})}$		ΔP_{Q}	
	O–H	H–O–H	O–H	H–O–H	O–H	H–O–H	O–H	H–O–H
cc-pVDZ					0.00035	–0.029	–0.00004	0.005
aug-cc-pCVDZ	0.96598	103.892	0.00004	–0.001	0.00044	–0.041		
aug-cc-pCVTZ	0.96063	104.230	–0.00006	0.005	0.00037	–0.038		
aug-cc-pCVQZ	0.95817	104.420	–0.00007	0.005				
aug-cc-pCV5Z	0.95757	104.487						
aug-cc-pCV6Z	0.95747	104.508						
Error	0.00010	0.020	0.00001	0.001	0.00006	0.004	0.00004	0.005

Table S2. Theoretical estimates for the O–H bond length and the H–O–H bond angle in H₃O⁺. The best estimates are obtained as the sum of the bold-faced values. Bond lengths and angles are given in Ångströms and degrees, respectively.

Basis set	$P_{\text{DKH/CCSD(T)}}$		ΔP_{T}		$\Delta P_{\text{(Q)}}$		ΔP_{Q}	
	O–H	H–O–H	O–H	H–O–H	O–H	H–O–H	O–H	H–O–H
cc-pVDZ					0.00032	–0.026	–0.00004	0.004
aug-cc-pCVDZ	0.98269	110.880	0.00005	0.000	0.00032	–0.036		
aug-cc-pCVTZ	0.97826	111.524	–0.00004	0.005	0.00025	–0.032		
aug-cc-pCVQZ	0.97572	111.834	–0.00004	0.004				
aug-cc-pCV5Z	0.97509	111.954						
aug-cc-pCV6Z	0.97501	111.982						
Error	0.00007	0.028	0.00001	0.001	0.00006	0.004	0.00004	0.004

Table S3. HF and correlation contributions to the proton affinity of the water molecule. The best estimate for the PA is obtained as the sum of the bold-faced values in this table and Table 4. All values are in kJ mol^{-1} . aug-cc-pCV(X,Y)Z means that the corresponding contributions were obtained by basis set extrapolation using the aug-cc-pCVXZ and aug-cc-pCVYZ basis sets.

Basis set	PA_{HF}	ΔPA_{MP2}	ΔPA_{CCSD}	$\Delta PA_{(\text{T})}$	ΔPA_{T}	$\Delta PA_{(\text{Q})}$	ΔPA_{Q}	ΔPA_{P}
cc-pVDZ	748.29	3.27	4.31	0.36	0.03	-0.16	0.02	-0.01
aug-cc-pCVDZ	726.26	-19.65	8.18	-2.45	-0.06	-0.30	0.06	
aug-cc-pCVTZ	733.65	-21.62	9.17	-3.60	0.11	-0.29		
aug-cc-pCVQZ	734.67	-22.18	9.49	-3.79	0.14			
aug-cc-pCV5Z	734.84	-22.51	9.69	-3.85				
aug-cc-pCV6Z	734.86	-22.79	9.85	-3.88				
aug-cc-pCV7Z	734.86	-22.99						
aug-cc-pCV(D,T)Z	734.26	-22.45	9.59	-4.09	0.18			
aug-cc-pCV(T,Q)Z	734.80	-22.59	9.73	-3.93	0.17			
aug-cc-pCV(Q,5)Z	734.87	-22.86	9.90	-3.92				
aug-cc-pCV(5,6)Z	734.86	-23.17	10.07	-3.92				
aug-cc-pCV(6,7)Z	734.86	-23.34						
Error	0.00	0.17	0.17	0.00	0.00	0.01	0.06	0.01

Table S4. Diagonal Born–Oppenheimer and relativistic corrections to the proton affinity of water. All values are in kJ mol^{-1} . The error of 0.10 kJ mol^{-1} given for $\Delta PA_{\text{DCG/HF}}$ is estimated error stemming from the neglect of the full Breit-operator as well as quantum electrodynamic corrections.

Basis set	$\Delta PA_{\text{DBOC/CCSD}}$	$\Delta PA_{\text{DBOC/T}}$	$\Delta PA_{\text{DKH/HF}}$	$\Delta PA_{\text{DC/HF}}$	$\Delta PA_{\text{DCG/HF}}$	$\Delta PA_{\text{DKH(T)}}$	$\Delta PA_{\text{DC(T)}}$	$\Delta PA_{\text{DCG(T)}}$
aug-cc-pCVDZ	-0.14	0.00	-0.28	-0.01	-0.05	-0.02	0.00	0.00
aug-cc-pCVTZ	-0.13	0.00	-0.28	-0.01	-0.05	-0.01	0.00	0.00
aug-cc-pCVQZ	-0.13		-0.28	-0.01	-0.05	-0.01		
aug-cc-pCV5Z			-0.27	-0.01	-0.05			
aug-cc-pCV6Z								
aug-cc-pCV7Z								
Error	0.00	0.00	0.00	0.00	0.10	0.00	0.00	0.00